Valence−Rydberg Bonding in Bimolecular R−$Ca^{+\bullet}NH_2$−R′ Complexes

Anthony E. Ketvirtis and Jack Simons*

Contribution from the Chemistry Department, University of Utah, Salt Lake City, Utah 84112

Received August 16, 1999. Revised Manuscript Received November 2, 1999

Abstract: Ab initio molecular orbital calculations were performed on species associated with the bimolecular reaction of protonated methylamine ($CH_3NH_3^+$) with methylcalcium ($CaCH_3$) to form the valence−Rydberg bonded complex $H_3CH_3N^{\bullet+}CaCH_3$. Gradient geometry optimizations and frequency calculations were performed at levels of theory up to and including UMP2(full)/6-311G(d,p) augmented by diffuse functions on the nitrogen atom. The complex $H_3CH_3N^{\bullet+}CaCH_3$ is bound by 9.77 kcal mol^{-1} relative to reactants at the projected second-order Möller−Plesset perturbation theory (PMP2) level, and both the charge and unpaired spin densities are delocalized between calcium and the adjacent amino group, the region of the valence−Rydberg bond. A rearranged product, $[H_3CH_2N{:}\rightarrow CaH\cdots CH_3]^{+\bullet}$, lies 12.38 kcal mol^{-1} below the valence−Rydberg complex, and is bound by 9.66 kcal mol^{-1} relative to dissociation products $[H_3CH_2N{:}\rightarrow CaH]^+ + \bullet CH_3$. The rearranged species is a distonic ion, with the positive charge mainly on calcium, and the unpaired electron on the carbon atom of the quasi-planar CH_3 moiety. A transition structure interconverting the two isomers lies ca. 21 kcal mol^{-1} above the higher-energy isomer, but is far above the dissociation limits of either species. Thus, in the gas phase at thermal energies, the valence−Rydberg complex and the lower-energy isomer $[H_3CH_2N{:}\rightarrow CaH\cdot\cdot\cdot CH_3]^{+\bullet}$ will not interconvert through this transition state.

I. Introduction

For many years, our research group has been involved in the study of molecular anionic species,[1] many of which contain outer electrons in diffuse loosely bound Rydberg-like orbitals.[1g] Rydberg orbitals also are important in the description of neutral species such as H_3O[2] and NH_4[1g,2b,e,f,h,3] (which Herzberg termed[2j] Rydberg molecules) and have been found to be crucial in describing valence−Rydberg bonding in short-lived neutral species such as $(NH_4)_2$[4] and NH_4Na,[5] and daughter cations such as $(NH_4)_2^+$.[4a,b]

Early experimental research by Garvey and Bernstein[6] provided evidence for the existence of $(NH_4)_2^+$, and was followed by theoretical studies, and interpretation of these data, by Evleth and co-workers.[7] More recently, the concept of bonding between Rydberg orbitals and outer valence orbitals in alkali metal atoms [e.g., (NH_4) bonded to Li, Na, or K] has been explored,[5] and such "mixed Rydberg-valence" bonds have been found to have bond strengths of between 11 and 16 kcal mol^{-1}. However, in these studies it was discovered that activation barriers leading, for example, to decompositions of $Na(NH_4)$ and $K(NH_4)$ to NH_3 + alkali hydride fragments are only 1 to 4 kcal mol^{-1} [$Li(NH_4)$ does not even have a barrier to dissociation to NH_3 + LiH], thus rendering these *neutral* species very unlikely to be easily probed experimentally.

In the case of the ammonium dimer, the cationic (one-electron-bonded) species $(NH_4)_2^+$ was found to be more strongly bound than the neutral (two-electron-bonded) $(NH_4)_2$,[4a,b] which is analogous to bond-strength trends seen in the alkali dimer neutrals and their cations.[8] Furthermore, whereas the neutral species is unstable to dissociation to $H_2 + 2NH_3$ (this process must overcome an activation barrier of ca. 2 kcal mol^{-1} before exothermic dissociation; on inclusion of zero-point vibrational energy, this barrier disappears),[4c] $(NH_4)_2^+$ fragmentation is endothermic to all dissociation products.[4a,b,9] For this reason, in the present effort, we have chosen to investigate, theoretically, the possibility of forming valence−Rydberg bonds in cationic species in which one-electron bonds may be involved.

As noted above, our earlier studies of valence−Rydberg bound molecules and cations involved nonsubstituted NH_4^+ and

(1) See, for example, (a) Simons, J.; Smith, W. D. *J. Chem. Phys.* **1973**, *58*, 4899. (b) Griffing, K.; Kenney, J.; Simons, J.; Jordan, K. *J. Chem. Phys.* **1975**, *63*, 4073. (c) Simons, J. *Annu. Rev. Phys. Chem.* **1977**, *28*, 15. (d) Simons, J. In *Theoretical Chemistry: Advances and Perspectives*; Eyring, H., Henderson, D., Eds.; Academic Press: New York, 1978; Vol. 3, p. 1. (e) Simons, J. *Int. J. Quantum Chem. Symp.* **1982**, *16*, 575. (f) Simons, J.; Jordan, K. D. *Chem. Rev.* **1987**, *87*, 535. (g) Simons, J.; Gutowski, M. *Chem. Rev.* **1991**, *91*, 669, and references therein. (h) Gutowski, M.; Skurski, P.; Jordan, K. D.; Simons, J. *Int. J. Quantum Chem.* **1997**, *64*, 183. (i) Simons, J. In *Photoionization and Photodetachment*; Ng, C. Y., Ed.; World Scientific Publishing Co.: Singapore, 1999.

(2) Ketvirtis, A. E.; Simons, J. *J. Phys. Chem. A* **1999**, in press. (b) Gutowski, M.; Simons, J. *J. Chem. Phys.* **1990**, *93*, 3874. (c) Talbi, D.; Saxon, R. *J. Chem. Phys.* **1989**, *91*, 2376. (d) Niblaeus, K. S. E.; Roos, B. O.; Siegbahn, P. E. M. *Chem. Phys.* **1977**, *25*, 207. (e) Wang, J.; Boyd, R. J. *Can. J. Phys.* **1994**, *72*, 851. (f) Raynor, S.; Herschbach, D. R. *J. Phys. Chem.* **1982**, *86*, 3592. (g) McLoughlin, P. W.; Gellene, G. I. *J. Phys. Chem.* **1992**, *96*, 4396. (h) Demolliens, A.; Eisenstein, O.; Hiberty, P. C.; Lefour, J. M.; Ohanessian, G.; Shaik, S. S.; Volatron, F. *J. Am. Chem. Soc.* **1989**, *111*, 5623. (i) Gellene, G. I.; Porter, R. F. *J. Chem. Phys.* **1984**, *81*, 5570. (j) Herzberg, G. *Annu. Rev. Phys. Chem.* **1987**, *38*, 27.

(3) (a) Boldyrev, A. I.; Simons, J. *J. Chem. Phys.* **1992**, *97*, 6621. (b) Herzberg, G. *Faraday Discuss. Chem. Soc.* **1981**, *71*, 165. (c) Watson, J. K. G.; Majewski, W. A.; Glownia, J. H. *J. Mol. Spectrosc.* **1986**, *115*, 82. (d) Ashfold, M. N. R.; Bennett, C. L.; Dixon, R. N.; Fielden, P.; Rieley, H.; Stickland, R. J. *J. Mol. Spectrosc.* **1986**, *117*, 216. (e) McMaster, B. N.; Mrozek, J.; Smith, V. H., Jr. *Chem. Phys.* **1982**, *73*, 131. (f) Kaspar, J.; Smith, V. H., Jr.; McMaster, B. N. *Chem. Phys.* **1985**, *96*, 81. (g) Havriliak, S.; King, H. F. *J. Am. Chem. Soc.* **1983**, *105*, 4. (h) Cardy, H.; Liotard, D.; Dargelos, A.; Poquet, C. *Chem. Phys.* **1983**, *77*, 287. (i) Kassab, E.; Evleth, E. M. *J. Am. Chem. Soc.* **1987**, *109*, 1653.

(4) (a) Boldyrev, A. I.; Simons, J. *J. Phys. Chem.* **1992**, *96*, 8840. (b) Boldyrev, A. I.; Simons, J. *J. Phys. Chem.* **1993**, *97*, 1470. (c) Wright, J. S.; McKay, D. *J. Phys. Chem.* **1996**, *100*, 7392.

(5) Boldyrev, A. I.; Simons, J. *J. Phys. Chem. A* **1999**, *103*, 3575.

(6) Garvey, J. F.; Bernstein, R. B. *Chem. Phys. Lett.* **1988**, *143*, 13.

(7) Kassab, E.; Fouquet, J.; Erleth, E. M. *Chem. Phys. Lett.* **1988**, *153*, 522.

10.1021/ja992969x CCC: $19.00
Published on Web 12/31/1999

H_3O^+ cations and neutral alkali atoms. Because we are interested in designing new molecules that use valence−Rydberg bonds to "link" fragments together into larger chains, cycles, and other topological moieties, we need to extend our choices both of the Rydberg and valence species. In the present effort, we chose to extend the Rydberg species by replacing NH_4^+ by a protonated amine RNH_3^+ and to replace the alkali atom by an alkyl-calcium radical R′Ca. These choices have also been influenced by the relative electronegativities of the constituent bonding sites. Specifically, sufficiently strong and covalent valence−Rydberg bonds can be formed only if the valence binding site is not so electronegative as to strip the Rydberg orbital of any electron(s) to form ionic bonds.

Calcium-containing polyatomic species have been the subjects of considerable gas-phase experimental[10] and theoretical[10x,11] interest, most notably in laser spectroscopic studies by Bernath and co-workers,[10a−o] and by Coxon and co-workers,[10q,aa−hh] so considerable data are available to which we can compare our computational findings. We have calculated Mulliken electronegativities {defined in terms of the ionization energy (IE) and electron affinity (EA) as $\chi = (1/2)[(IE + EA)/3.15]$} for the radical-center orbital in $CaCH_3$ ($\chi = 0.935$), and for the Rydberg orbital of NH_4 ($\chi = 0.7$). The difference in these two electronegativities is sufficiently small to suggest that valence−Rydberg covalent bonding is plausible in the species examined in this work. In this regard, then, we have performed ab initio molecular orbital (MO) calculations to study the feasibility of forming valence−Rydberg bonds resulting from the complexation of protonated methylamine ($CH_3NH_3^+$) with methylcalcium ($CaCH_3$) to form a one-electron bond.

II. Methods

Our ab initio calculations were performed using the Gaussian 94[12] and Gaussian 98[13] series of programs, on an IBM RISC System/6000 computer and on an SGI Origin 2000 computer at the Utah Center for High Performance Computing, both at the University of Utah. In all calculations, we have used a standard Gaussian triple split-valence 6-311G(d,p) basis set,[14] augmented by a group of four extra sets of s-type functions, two extra sets of p-type functions, and one extra set of d-type functions on the nitrogen atom. This extra group of diffuse basis functions was formed by modifying the set developed by Gutowski and Simons[2b] for Rydberg neutral and anionic species; the final set of augmented primitive basis functions has been reported elsewhere.[2a] The 6-311G(d,p) basis set for calcium[15] was obtained from the Pacific Northwest National Laboratory library.[16]

Geometry optimizations were performed using gradient techniques[17] with the augmented basis set at levels of theory from Hartree−Fock (spin-restricted or RHF[18] for closed-shell species; spin-unrestricted or UHF[19] for open-shell species) and with inclusion of electron correlation to second-order Møller−Plesset perturbation theory[20,21] [RMP2(full)

(8) See, for example, (a) Zemke, W. T.; Stualley, W. C. *J. Phys. Chem.* **1993**, *97*, 2053. (b) Barakat, B.; Bacis, R.; Carrot, F.; Churrassy, S.; Crozet, P.; Martin, F. *Chem. Phys.* **1986**, *102*, 215. (c) Hessel, M. M.; Vidal, C. R. *J. Chem. Phys.* **1979**, *70*, 4439. (d) Schmidt-Mink, I.; Müller, W.; Meyer, W. *Chem. Phys.* **1985**, *92*, 263. (e) Kaldor, U. *Chem. Phys.* **1990,** *140*, 1. (d) Sun, Z.; Barnett, R. N.; Lester, W. A., Jr. *Chem. Phys. Lett.* **1992**, *195*, 365. (f) Bernheim, R. A.; Gold, L. P.; Tipton, T.; Konowalow, D. D. *Chem. Phys. Lett.* **1984**, *105*, 201. (g) Bernheim, R. A.; Gold, L. P.; Tipton, T. *J. Chem. Phys.* **1983**, *78*, 3635. (h) Bernheim, R. A.; Gold, L. P.; Tipton, T. *Chem. Phys. Lett.* **1982**, *92*, 13. (i) McGeoch, M. W.; Schlier, R. E. *Chem. Phys. Lett.* **1983**, *99*, 347. (j) Konowalow, D. D.; Fish, J. L. *Chem. Phys. Lett.* **1984**, *104*, 210. (k) Konowalow, D. D.; Rosenkrantz, M. E. *Chem. Phys. Lett.* **1979**, *61*, 489. (l) Jones, K. M.; Maleki, S.; Bize, S.; Lett, P. D.; Williams, C. J.; Richling, H.; Knöckel, H.; Tiemann, E.; Wang, H.; Gould, P. L.; Stwalley, W. C. *Phys. Rev. A* **1996**, *54*, R1006. (m) Zemke, W. T.; Stwalley, W. C. *J. Chem. Phys.* **1994**, *100*, 2661. (n) Müller, W.; Meyer, W. *J. Chem. Phys.* **1984**, *80*, 3311. (o) Partridge, H.; Bauschlicher, C. W., Jr.; Walch, S. P.; Liu, B. *J. Chem. Phys.* **1983**, *79*, 1866. (p) Magnier, S.; Millié, P.; Dulieu, O.; Masnou-Seeuws, F. *J. Chem. Phys.* **1993**, *98*, 7113. (q) Bordas, C.; Labastie, P.; Chevaleyre, J.; Broyer, M. *Chem. Phys.* **1989**, *129*, 21. (r) Nitz, D. E.; Hogan, P. B.; Schearer, L. D.; Smith, S. J. *J. Phys. B* **1979**, *12*, L103. (s) Bähring, A.; Hertel, I. V.; Meyer, E.; Meyer, W.; Spies, N.; Schmidt, H. *J. Phys. B* **1984**, *17*, 2859. (t) Amiot, C.; Vergès, J.; Fellows, C. E. *J. Chem. Phys.* **1995**, *103*, 3350. (u) Zemke, W. T.; Tsai, C.-C.; Stwalley, W. C. *J. Chem. Phys.* **1994**, *101*, 10382. (v) Heinze, J.; Engelke, F. *J. Chem. Phys.* **1988**, *89*, 42. (w) Ilyabayev, E.; Kaldor, U. *J. Chem. Phys.* **1993,** *98*, 7126. (x) Magnier, S.; Millié, P. *Phys. Rev. A* **1996**, *54*, 204. (y) Jeung, G.-H.; Ross, A. J. *J. Phys. B* **1988**, *21*, 1473. (z) Broyer, M.; Chevaleyre, J.; Delacretaz, G.; Martin, S.; Wöste, L. *Chem. Phys. Lett.* **1983**, *99*, 206.

(9) See ref 13 cited in ref 5.

(10) (a) Bernath, P. F. *Adv. Photochem.* **1997**, *23*, 1, and references therein. (b) Morbi, Z.; Zhao, C.; Bernath, P. F. *J. Chem. Phys.* **1997**, *106*, 4860. (c) Morbi, Z.; Zhao, C.; Bernath, P. F. *J. Chem. Phys.* **1997**, *107*, 1297. (d) Bopegedra, A. M. R. P.; Brazier, C. R.; Bernath, P. F. *J. Mol. Spectrosc.* **1988**, *129*, 268. (e) Bopegedra, A. M. R. P.; Brazier, C. R.; Bernath, P. F. *Chem. Phys. Lett.* **1987**, *136*, 97. (f) Brazier, C. R.; Bernath, P. F. *J. Chem. Phys.* **1987**, *86*, 5918. (g) O'Brien, L. C.; Bernath, P. F. *J. Am. Chem. Soc.* **1986**, *108*, 5017. (h) O'Brien, L. C.; Brazier, C. R.; Kinsey-Nielsen, S.; Bernath, P. F. *J. Phys. Chem.* **1990**, *94*, 3543. (i) Bopegedra, A. M. R. P.; Fernando, W. T. M. L.; Bernath, P. F. *J. Phys. Chem.* **1990**, *34*, 3547. (j) Brazier, C. R.; Bernath, P. F. *J. Chem. Phys.* **1989**, *91*, 4548. (k) Bernath, P. F.; Brazier, C. R. *Astrophys. J.* **1985**, *288*, 373. (l) Jarman, C. N.; Bernath, P. F. *J. Chem. Phys.* **1993**, *98*, 6697. (m) Jarman, C. N.; Bernath, P. F. *J. Chem. Phys.* **1992**, *97*, 1711. (n) Fernando, W. T. M. L.; Ram, R. S.; O'Brien, L. C.; Bernath, P. F. *J. Phys. Chem.* **1991**, *95*, 2665. (o) Brazier, C. R.; Ellingboe, L. C.; Kinsey-Nielsen, S.; Bernath, P. F. *J. Am. Chem. Soc.* **1986**, *108*, 2126. (p) Hilborn, R. C.; Qingshi, Z.; Harris, D. O. *J. Mol. Spectrosc.* **1983**, *97*, 73. (q) Li. M.; Coxon, J. A. *J. Mol. Spectrosc.* **1996**, *176*, 206. (r) Wormsbecher, R. F.; Trkula, M.; Martner, C.; Penn, R. E.; Harris, D. O. *J. Mol. Spectrosc.* **1983**, *97*, 29. (s) Marr, A. J.; Tanimoto, M.; Goodridge, D.; Steimle, T. C. *J. Chem. Phys.* **1995**, *103*, 4466. (t) Pullins, S. H.; Reddic, J. E.; France, M. R.; Duncan, M. A. *J. Chem. Phys.* **1998**, *108*, 2725. (u) Scurlock, C. T.; Pullins, S. H.; Reddic, J. E.; Duncan, M. A. *J. Chem. Phys.* **1996**, *104*, 4591. (v) Pullins, S. H.; Scurlock, C. T.; Reddic, J. E.; Duncan, M. A. *J. Chem. Phys.* **1996**, *104*, 7518. (w) Scurlock, C. T.; Pullins, S. H.; Duncan, M. A. *J. Chem. Phys.* **1996**, *105*, 3579. (x) Kochanski, E.; Constantin, E. *J. Chem. Phys.* **1987**, *87*, 1661. (y) Anderson, M. A.; Ziurys, L. M. *Astrophys. J.* **1995**, *444*, L57. (z) Keller, A.; Lawruszczuk, R.; Soep, B.; Visticot, J. P. *J. Chem. Phys.* **1996**, *105*, 4556. (aa) Coxon, J. A.; Li, M.; Presunka, P. I. *J. Mol. Spectrosc.* **1991**, *150*, 33. (bb) Li, M.; Coxon, J. A. *Can. J. Phys.* **1994**, *72*, 1200. (cc) Coxon, J. A.; Li, M.; Presunka, P. I. *J. Mol . Spectrosc.* **1994**, *164*, 118. (dd) Coxon, J. A.; Li. M.; Presunka, P. I. *Mol. Phys.* **1992**, *76*, 1463. (ee) Li, M.; Coxon, J. A. *J. Chem. Phys.* **1992**, *97*, 8961. (ff) Li, M.; Coxon, J. A. *J. Chem. Phys.* **1995**, *102*, 2663. (gg) Li, M.; Coxon, J. A. *J. Chem. Phys.* **1996**, *104*, 4961. (hh) Li, M.; Coxon, J. A. *J. Mol. Spectrosc.* **1999**, *196*, 14.

(11) (a) Kirschner, K. N.; Bowen, J. P.; Duncan, M. A. *Chem. Phys. Lett.* **1998**, *295*, 204. (b) Chan, W.-T.; Hamilton, I. P. *Chem. Phys. Lett.* **1998**, *297*, 217. (c) Bauschlicher, C. W., Jr.; Sodupe, M.; Partridge, H. *J. Chem. Phys.* **1992**, *96*, 4453. (d) Kaupp, M.; Schleyer, P. v. R.; Stoll, H.; Preuss, H. *J. Chem. Phys.* **1991**, *94*, 1360. (e) Kaupp, M.; Schleyer, P. v. R.; Stoll, H.; Preuss, H. *J. Am. Chem. Soc.* **1991**, *113*, 6012. (f) Seijo, L.; Baradiarán, Z.; Huzinaga, S. *J. Chem. Phys.* **1991**, *94*, 3762. (g) Ref 97 cited in ref 10(a). (h) Ortiz, J. V. *J. Chem. Phys.* **1990**, *92*, 6728.

(12) GAUSSIAN 94, Revision B.1; Frisch, M. J.; Truck, G. W.; Schlegel, H. B.; Gill, P. M. W.; Johnson, B. G.; Robb, M. A.; Cheeseman, J. R.; Keith, T.; Petersson, G. A.; Montgomery, J. A.; Raghavachari, K.; Al-Laham, M. A.; Zakrzewski, V. G.; Ortiz, J. V.; Foresman, J. B.; Cioslowski, J.; Stefanov, B. B.; Nanayakkara, A.; Challacombe, M.; Peng, C. Y.; Ayala, P. Y.; Chen, W.; Wong, M. W.; Andres, J. L.; Replogle, E. S.; Gomperts, R.; Martin, R. L.; Fox, D. J.; Binkley, J. S.; Defrees, D. J.; Baker, J.; Stewart, J. P.; Head-Gordon, M.; Gonzalez, C.; Pople, J. A. Gaussian, Inc.: Pittsburgh, PA, 1995.

(13) GAUSSIAN 98, Revision A.6; Frisch, M. J.; Trucks, G. W.; Schlegel, H. B.; Scuseria, G. E.; Robb, M. A.; Cheeseman, J. R.; Zakrzewski, V. G.; Montgomery, J. A., Jr.; Stratmann, R. E.; Burant, J. C.; Dapprich, S.; Millam, J. M.; Daniels, A. D.; Kudin, K. D.; Strain, M. C.; Farkas, O.; Tomasi, J.; Barone, V.; Cossi, M.; Cammi, R.; Menucci, B.; Pomelli, C.; Adamo, C.; Clifford, S.; Ochterski, J.; Petersson, G. A.; Ayala, P. Y.; Cui, Q.; Morokuma, K.; Malick, D. K.; Rabuck, A. D.; Raghavachari, K.; Foresman, J. B.; Cioslowski, J.; Ortiz, J. V.; Stefanov, B. B.; Liu, G.; Liashenko, A.; Piskorz, P.; Komaromi, I.; Gomperts, R.; Martin, R. L.; Fox, D. J.; Keith, T.; Al-Laham, M. A.; Peng, C. Y.; Nanayakkara, A.; Gonzalez, C.; Challacombe, M.; Gill, P. M. W.; Johnson, B.; Chen, W.; Wong, M. W.; Andres, J. L.; Gonzalez, C.; Head-Gordon, M.; Replogle, E. S.; Pople, J. A. Gaussian, Inc.: Pittsburgh, PA, 1998.

(14) Krishnan, R.; Frisch, M. J.; Pople, J. A. *J. Chem. Phys.* **1980**, *72*, 4244.

(15) Blaudeau, J.-P.; McGrath, M. P.; Curtiss, L. A.; Radom, L. *J. Chem. Phys.* **1997**, *107*, 5016.

Table 1: Spin, Relative Energies, and Zero-Point Energies of $R-Ca^{+\bullet}NH_2-R'$ Complexes and Dissociation Products[a]

species	$\langle S^2 \rangle$ HF/MP2	ZPE[b]	ZPE[c]	relative energy wrt. **4**
1		47.09	47.97	
2	0.753/0.753	18.96	19.50	
1 + 2	0.753/0.753	66.05	67.47	+22.15
3	0.754/0.754	66.35	67.51	+12.38
4	0.759/0.759	60.34	62.24	0.00
5		41.70	42.71	
6	0.761/0.762	17.10	17.79[d]	
5 + 6	0.761/0.762	58.80	60.50	+9.66
7	1.328/1.328	60.18	61.10	+33.36

[a] In kcal mol^{-1}; scaled ZPE included. [b] At SCF optimized geometries unless otherwise stated; scaled by 0.89.[2a] [c] At UMP2 optimized geometries unless otherwise stated; scaled by 0.89.[2a] [d] Scaled by 0.94.[22]

or UMP2(full), as appropriate]. Transition structure searches were performed by gradient optimizations using the CALCALL[12,13] technique, and harmonic frequency calculations for species at critical points were performed both at HF and at MP2 levels of theory, from which zero-point vibrational energies (ZPE) also were obtained. ZPE values from self-consistent field (SCF)-level calculations are reported in Table 1, scaled by a factor of 0.89;[2a] UMP2-level ZPE values also are reported in Table 1, scaled by a factor of 0.95 for nitrogen-containing species[2a] and 0.94 for non-N-containing compounds.[22] In addition, for transition structures (TS), the forces on the nuclei associated with the normal modes of vibration of imaginary frequencies were used to determine the identities of the local minimum structures connecting to the TS. The total energies obtained for each species are given in Table 1, and their relative energies at the PMP2 (spin-projection included)[23] level are summarized in Figure 1.

Figure 2 displays optimized geometric parameters of the species under study, both at the SCF level and at the UMP2 level, with the augmented basis set described earlier in this section. The large number of bond lengths and bond angles associated with many of these structures makes a detailed listing of each geometric parameter impractical. Therefore, we have omitted bond lengths involving hydrogen atoms as well as some bond angles involving methyl- or amino-hydrogens, except in cases where they are relevant in describing an isomerization or an unusual bonding arrangement. The parameters that have been omitted have values at or near those of "conventional" tetrahedral carbon- or nitrogen-containing species. Finally, full details on the geometries of all species are included in the Cartesian coordinates offered as Supporting Information.

In addition, (Mulliken) charge- and spin-density information, obtained at the MP2-level optimized geometries, is provided in Figure 2, and pictorial representations of some of the higher-filled bonding molecular orbitals, particularly those associated with valence−Rydberg bonds, are given in Figures 3−7 in MOLDEN[24] format.

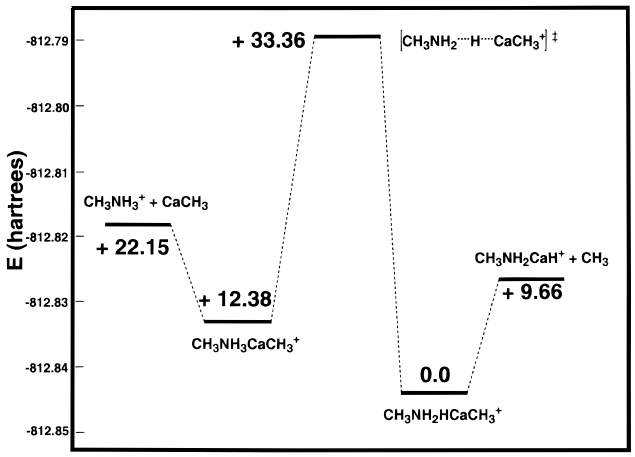

Figure 1. Total electronic and relative energies of species **3** and **4**, transition structure **7**, and lowest-energy dissociation products at the PMP2 level of theory with the augmented basis set described in Section II. Total energies are given in hartrees without inclusion of ZPE; relative energies are given in kcal mol^{-1} with scaled ZPE included.

III. Results

A. One-Electron Valence−Rydberg-Bonded Structures. 1. SCF-Level. In the gas phase, the reactants discussed here can, in principle, approach each other in a variety of orientations, including one in which the four "heavy" atoms are aligned in a collinear fashion. Our first attempt, therefore, at locating a local minimum structure on the ground potential energy surface (PES) involved a search for such a linear, or quasi-linear, bimolecular reaction product. Although we located such a critical point on this surface having an energy lying below that of separated $CH_3NH_3^+ + CaCH_3$ by ca. 6.34 kcal mol^{-1} (scaled ZPE included), a vibrational frequency analysis yielded two imaginary frequencies (31i cm^{-1} and 24i cm^{-1}), both of which are associated with bending motions of the Ca−N−C angle from the optimized value of 172.6°.

Allowing this complex to bend yielded a stable complex (species **3**; see Figure 2, where structures of all species examined here are shown) that is similar in geometry to the aforementioned quasi-linear compound, but with a significantly bent Ca−N−C angle (117.4°). This complex lies only 0.73 kcal mol^{-1} below the quasi-linear species, so **3** is bound by ca. 7.07 kcal mol^{-1} relative to $CH_3NH_3^+ + CaCH_3$ (scaled ZPE included) at this level of theory. A subsequent frequency calculation on the optimized geometry yielded one imaginary frequency (1i cm^{-1}) associated with essentially barrierless rotation of the methyl H atoms about the Ca−C bond. Thus, the effect of this instability on the total energy, and on our interpretation, of species **3** is negligible. Clearly, the large radial and angular extent of both the diffuse Rydberg orbital on the substituted ammonium group and the outermost 4sp hybrid valence orbital on calcium (see Figure 3 for depictions of these orbitals) result in the formation of a complex whose energy is only weakly dependent on the Ca−N−C bond angle.

The optimized C−Ca bond length (2.405 Å) in **3** is only slightly shorter than that obtained for separated $Ca-CH_3$ (species **2** in Figure 2) (2.442 Å) and is similar to C−Ca distances obtained experimentally for ground-state (X^2A_1) Ca−

(16) For calcium: "Basis sets were obtained from the Extensible Computational Chemistry Environment Basis Set Database, Version 1.0, as developed and distributed by the Molecular Science Computing Facility, Environmental and Molecular Sciences Laboratory, which is part of the Pacific Northwest Laboratory, P.O. Box 999, Richland, WA 99352, and funded by the U. S. Department of Energy. The Pacific Northwest Laboratory is a multiprogram laboratory operated by Battelle Memorial Institute for the U. S. Department of Energy under contract DE-AC06-76RLO 1830. Contact David Feller or Karen Schuchardt for further information."

(17) Schlegel, H. B. *J. Comput. Chem.* **1982**, *3*, 214.

(18) (a) Roothaan, C. C. J. *Rev. Mod. Phys.* **1951**, *23*, 69. (b) Hall, G. G. *Proc. R. Soc. London Ser. A* **1951**, *205*, 541.

(19) (a) Roothaan, C. C. J. *Rev. Mod. Phys.* **1960**, *32*, 179. (b) Binkley, J. S.; Pople, J. A.; Dobosh, P. A. *Mol. Phys.* **1974**, *28*, 1423.

(20) (a) Møller, C.; Plesset, M. S. *Phys. Rev.* **1934**, *46*, 618. (b) Binkley, J. S.; Pople, J. A. *Int. J. Quantum Chem.* **1975**, *9*, 229.

(21) (a) Head-Gordon, M.; Pople, J. A.; Frisch, M. J. *Chem. Phys. Lett.* **1988**, *153*, 503. (b) Frisch, M. J.; Head-Gordon, M.; Pople, J. A. *Chem. Phys. Lett.* **1990,** *166*, 275. (c) Frisch, M. J.; Head-Gordon, M.; Pople, J. A. *Chem. Phys. Lett.* **1990,** *166*, 281. (d) Saebo, S.; Almlöf, J. *Chem. Phys. Lett.* **1989**, *154*, 83.

(22) Rodriquez, C. F.; Bohme, D. K.; Hopkinson, A. C. *J. Phys. Chem.* **1996**, *100*, 2942.

(23) (a) Schlegel, H. B. *J. Phys. Chem.* **1988**, *92*, 3075. (b) Schlegel, H. B. *J. Chem. Phys.* **1986**, *84*, 4530.

(24) Schaftenaar, G. MOLDEN 3.4, CAOS/CAMM Center, The Netherlands, 1998.

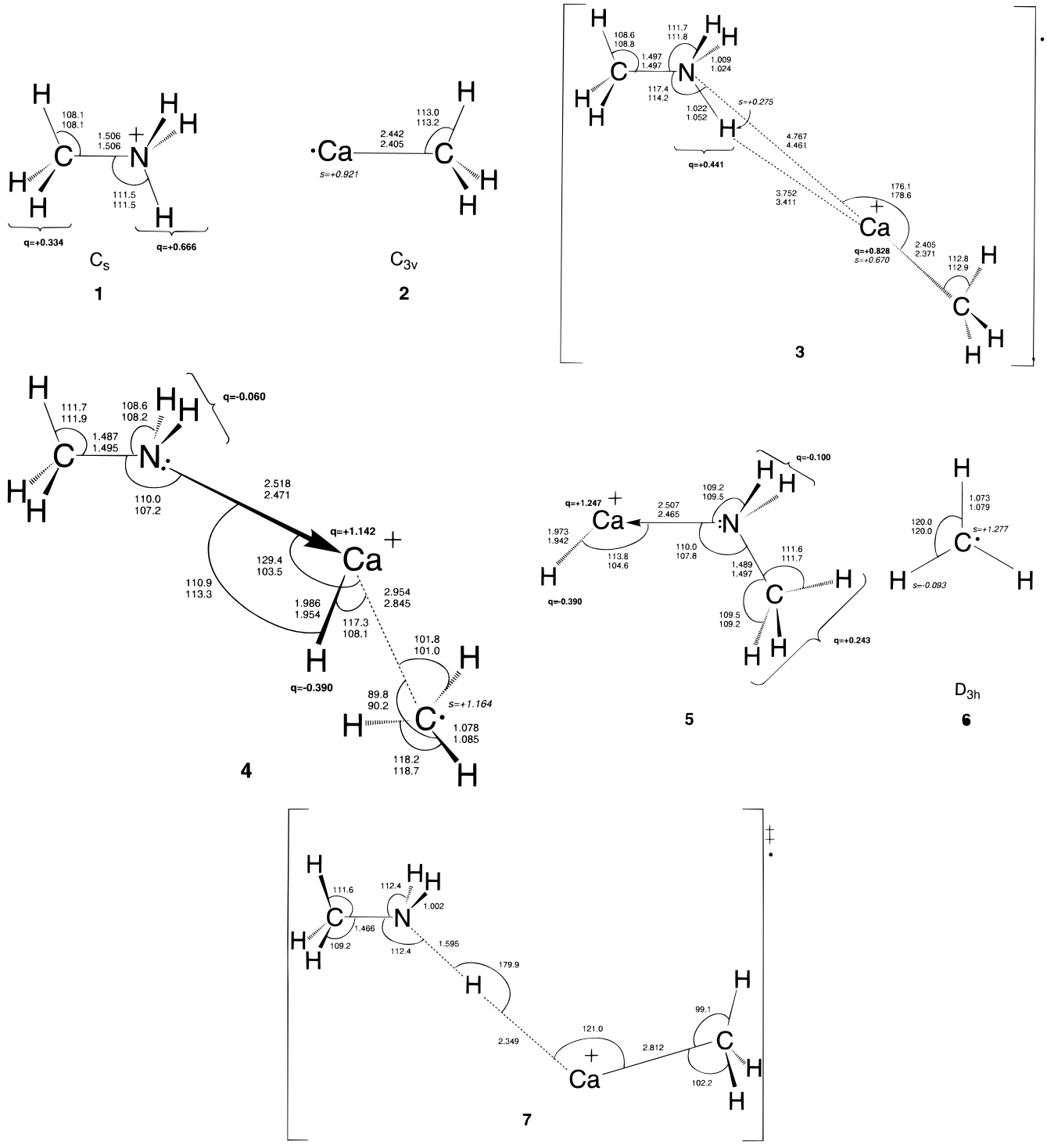

Figure 2. Structural parameters of species associated with our study of valence−Rydberg bonding. Bond lengths involving H atoms have been omitted except where deemed relevant to the description of rearrangement processes, and only selected bond lengths and angles have been included for the purpose of diagram clarity. Cartesian coordinates of all species studied are included in Supporting Information. Bond lengths are in Ångströms; bond angles are in degrees. Where one set of geometric parameters is listed, it denotes an optimized structure at the HF/6-311G(d,p) level of theory. Where two sets of geometric parameters are listed, the upper value denotes optimization at the HF/6-311G(d,p) level of theory; the lower value denotes optimization at the MP2(full)/6-311G(d,p) level of theory. In each case, these basis sets have been augmented by four sets of extra "s" functions, two sets of extra "p" functions, and one set of extra "d" functions on nitrogen. Atomic- and functional group Mulliken charges are listed in boldface type and are preceded by "q="; spin densities are listed in italics and are preceded by "s=". Both sets of data were obtained at UMP2-level optimized structures, with the basis set listed above.

CH_3 [(2.349 ± 0.013) Å][10a,j] and for ground-state ($X^2\Sigma^+$) Ca−CCH (2.349 Å),[10y] as well as those obtained theoretically for $CaCH_3$,[11b,h] CaCCH,[11b,g] and CaCN.[11b] The separation between calcium and nitrogen, the atomic centers between which valence−Rydberg bonding is being examined, is 4.767 Å at this level of theory. Such a distance is significantly longer than SCF-level valence−Rydberg X−N equilibrium distances for $X-NH_4$ species that we studied earlier, where X = K (4.121 Å)[5] or Na (3.645 Å).[5] Nevertheless, the existence of 7.1 kcal mol^{-1} binding energy vis-à-vis "reactants" **1** and **2** indicates

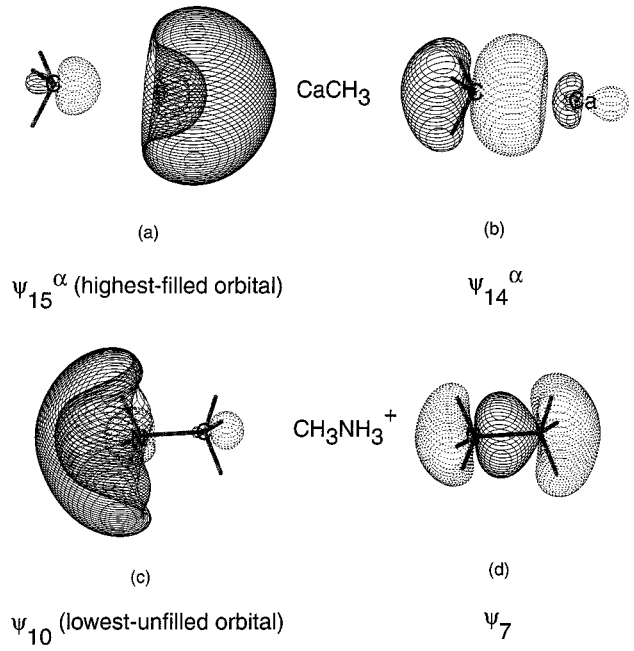

Figure 3. MOLDEN pictorial representations of (a) the 4sp hybrid valence orbital centered on Ca of $CaCH_3$ (species **1**); (b) the α-component of the Ca−C bond in **1**; (c) the Rydberg orbital centered on the −NH3 moiety of $CH_3NH_3^+$ (species **2**); (d) the N−C bond in **2**. All orbital diagrams for a given species show the atoms in the same orientation.

the presence of a weak bonding interaction between nitrogen and calcium in **3**.

Another noteworthy feature of structure **3** lies in the bonding between the ammonium nitrogen and the hydrogen atom oriented toward the calcium atom of the $CaCH_3$ group. This N−H bond length is 1.022 Å; the other two N−H bond lengths in this ammonium group are 1.009 Å, similar to that found in ammonia (1.012 Å).[25] Although the Ca−H distance still is large (3.752 Å), the one extended N−H distance suggests the possibility of a small bonding interaction between these H and Ca atoms. Indeed, as is discussed later, an isomer (**4**) of **3** in which this particular hydrogen atom forms a two-electron bond with Ca lies at a lower energy on the PES (see the structure of **4** in Figure 2 and its energy relative to other species in Table 1 and Figure 1).

2. MP2 Level. Subsequent MP2-level geometry optimization on species **3** produced a structure similar to that found at the SCF level, albeit slightly more compact (see Figure 2). The insensitivity of the total electronic energy to relatively large geometric distortions during the gradient optimization of **3** made impossible the calculation of an optimum geometry that satisfies all four criteria of convergence in the Berny optimization algorithm within Gaussian 98. Nevertheless, the energy did converge to within 10^{-5} hartrees, and a subsequent harmonic vibrational frequency calculation on the geometry of lowest energy yielded only one imaginary frequency of very small magnitude (1i cm^{-1}) associated with an energetically insignificant methyl hydrogen rotation about the C−Ca bond, similar to that noted at the SCF level of theory.

Species **3** is bound relative to $CH_3NH_3^+ + CaCH_3$ by 9.77 kcal mol^{-1} (scaled ZPE included) at the PMP2 level (see Table 1 and Figures 1 and 2), a value somewhat larger than the 7.07 kcal mol^{-1} calculated at the SCF level. We believe that the binding energy in **3** arises largely through the formation of a one-electron valence−Rydberg bond, although it is likely that charge−dipole- and charge−induced-dipole interactions also are present. To estimate the relative magnitudes of these contributions, we evaluated the binding energy of the neutral analogue to **3**, $CH_3NH_3CaCH_3$, a species for which charge−dipole-

(25) *Molecular Spectra and Molecular Structure III. Electronic Spectra and Electronic Structure of Polyatomic Molecules.* Van Nostrand Reinhold: New York, 1966.

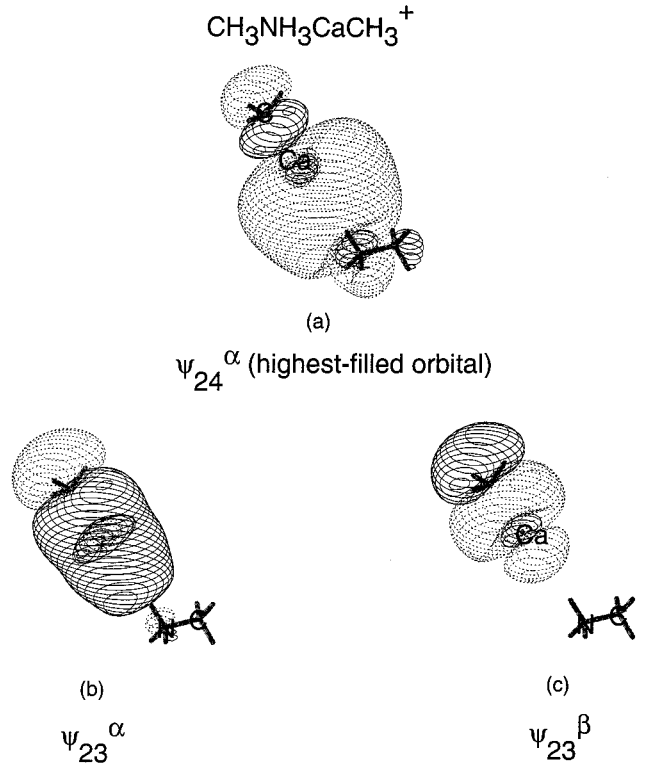

Figure 4. MOLDEN pictorial representations of (a) the Ca•NH_3-valence−Rydberg one-electron bond in species **3**; (b, c) the α- and β-components of the Ca−C two-electron bond in **3**. All orbital diagrams show the atoms in the same orientation.

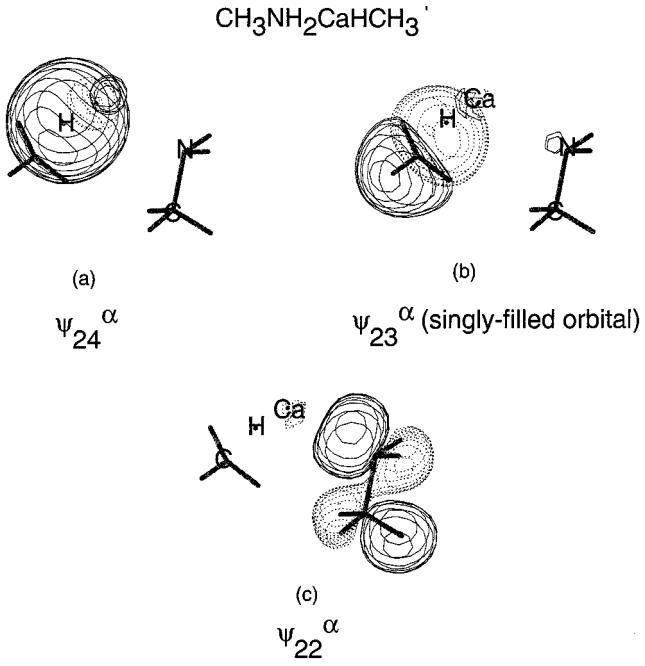

Figure 5. MOLDEN pictorial representations of (a) the α-component of the Ca−H bond of species **4**; (b) the singly filled p_π-orbital of the quasi−planar CH_3 moiety within **4**; (c) the α-component of the N:→Ca dative bond of **4**. All orbital diagrams show the atoms in the same orientation.

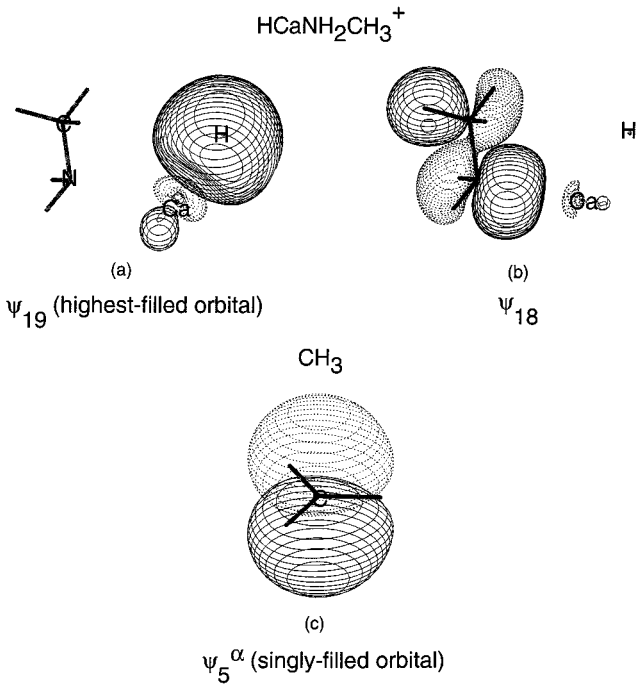

Figure 6. MOLDEN pictorial representations of (a) the Ca−H bond of species **5**; (b) the N:→Ca dative bond of **5**; (c) the singly filled p_π-orbital centered on carbon of species **6**. All orbital diagrams for a given species show the atoms in the same orientation.

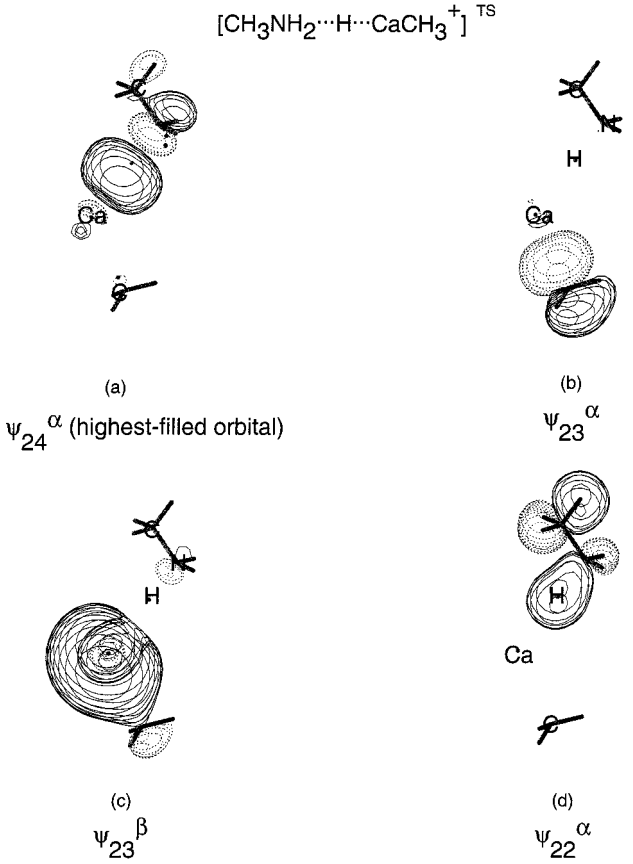

Figure 7. MOLDEN pictorial representations of (a) N−H- and valence−Rydberg bond breaking and Ca−H bond formation in transition structure **7**; (b) Ca−C bond cleavage and formation of a singly filled p_π-orbital of a quasi−planar CH_3 moiety in **7**; (c) Ca−C bond cleavage in **7**; (d) N−H bond breaking and formation of a N:→Ca dative bond in **7**. All orbital diagrams show the atoms in the same orientation.

and charge−induced-dipole interactions do not exist. In particular, we investigated the thermodynamics of the reaction $CH_3NH_3 + CaCH_3 \rightarrow CH_3NH_3CaCH_3$ by performing single-point MP2-level calculations, with the basis set defined in section II, on CH_3NH_3 and $CH_3NH_3CaCH_3$ at the MP2-optimized geometries of cations **1** and **3**, respectively. The spin-projected (where necessary) MP2 energies, together with that of MP2-optimized $CaCH_3$ (**2**), yielded a ΔE value of -20.48 kcal mol^{-1} (ZPE not included). This value represents the strength of the two-electron valence−Rydberg bond in $CH_3NH_3CaCH_3$. The greater strength of this bond compared to that of the one-electron bond formed in **3** is in marked contrast to the relative bond strengths in the ammonium dimer and alkali dimer neutrals and cations;[4a,b,8] nevertheless, this result reinforces our characterization of the one-electron Ca−N bond in **3** as resulting from a valence orbital−Rydberg orbital interaction.

Also noteworthy is the fact that the N−H bond involving the hydrogen atom oriented toward calcium is longer that the other two N−H bonds by nearly 0.03 Å, in a manner qualitatively similar to the results found at the SCF level. These results suggest, as discussed earlier, the possibility of a weak N−H bond and a small Ca−H bonding interaction. Indeed, an inspection of the spin density distribution also obtained in Figure 2 shows a significant delocalization between the Ca atom ($s = +0.670$) and the weakly bonded ammonium hydrogen ($s = +0.275$).

The covalent bonding characteristics of **3** further manifest themselves when comparing the charge and spin distributions of **3** with those of the fragments **1** and **2**, which carry the total net charge and spin densities, respectively, before complex formation. The -NH_3 group carries a charge of $+0.666$ in **1**, whereas in complex **3**, this same -NH_3 group has $q = 0.441$. This is consistent with ca. 0.22 units of an electron being transferred from fragment **2** to **1** when the bond is formed. The Ca atom has a spin density of $s = 0.921$ in **2**, whereas in complex **3**, its spin has decreased to $s = 0.670$. This again is consistent with ca. 0.25 units of an electron being transferred from **2** to **1** upon bond formation.

The inclusion of electron correlation at this level has resulted in the equilibrium length of the C−Ca bond (2.371 Å) being slightly shorter than that obtained at the SCF level; the MP2-optimized value is in even closer agreement with the spectroscopically derived[10a,j,y] and theoretically calculated[11b,g,h] C−Ca bond lengths discussed earlier.

Figure 3 shows depictions of the 4sp singly occupied and C−Ca orbitals of $CaCH_3$ and the (empty) Rydberg and N−C bonding orbitals of $CH_3NH_3^+$; Figure 4 displays the singly occupied Rydberg−valence and Ca−C bonding orbitals of **3**. The singly occupied orbital of **3** (ψ_{24}^α) contains a large lobe on Ca and a smaller, but significant, lobe on NH_3 combined in a constructive bonding manner. The origin of this bonding orbital can be seen clearly on inspection of ψ_{15}^α in Figure 3 (the singly filled 4s4p orbital based on Ca) and ψ_{10} (the unfilled diffuse Rydberg orbital on NH_3). The next-highest-filled orbitals of **3**, ψ_{23}^α and ψ_{23}^β, represent the two-electron Ca−C bond. These orbital pictures are consistent with the depiction of species **3** as containing a Ca−N one-electron valence−Rydberg bonding interaction in which the unpaired electron and the positive charge are delocalized over the calcium and Rydberg centers.

B. Rearranged Bimolecular Complexes and Transition Structures. *1. SCF-Level.* As discussed earlier, the optimized geometry of the complex formed from the addition of $CaCH_3$ to $CH_3NH_3^+$ contains an ammonium N−H bond for the hydrogen atom oriented toward the calcium that is longer than

the other two N−H bonds of this group. This observation has led us to consider the thermodynamic stability of **3** relative to an isomer in which there exists a Ca−H bond. A subsequent geometry optimization led to a structure for which there exists not only a Ca−H bond but also a variety of unusual bonding features. Furthermore, **4** lies 10.91 kcal mol^{-1} below **3**, and is the lower-energy isomer.

The structure of **4** contains a Ca−C distance (2.954 Å) considerably longer than that obtained from spectroscopic measurements[10a,j] and theoretical calculations[11b,h] on $CaCH_3$. Also, the Ca−N separation in **4** (2.518 Å) is approximately 0.4 Å longer than that obtained from spectroscopic[10a,b] studies on $CaNH_2$, and from theoretical calculations on $CaNH_2$,[11b,h] CaNCO,[11b,g] CaNNN,[11b,g] CaNCS,[11b,g] and CaNC,[11b,g] but is similar to that calculated for $Ca^{2+}\leftarrow{:}N{\equiv}N{:}$.[11a] Thus, **4** does not contain conventional Ca−C or Ca−N bonds; instead, it seems to involve a H−Ca$^+$ cation that is weakly complexed to a CH_3 radical and bound, in a dative manner, to a methylamine.

The identities of the lowest-energy dissociation products for species **4** are not obvious because either the dative N−Ca bond or the Ca−CH_3 interaction could be the weakest bond. We therefore studied three possible dissociation channels of **4** at both the SCF and MP2 levels of theory: $HCaNH_2CH_3^+$ (**5**) + CH_3 (**6**), $CH_3NH_2 + HCaCH_3^+$, and $CH_3NH_2 + CaH^+ + CH_3$. We found the respective dissociation limits to lie 8.17, 34.55, and 44.43 kcal mol^{-1} (scaled ZPE included) above **4** at the SCF level, and 9.66, 36.86, and 48.54 kcal mol^{-1} (scaled ZPE included) above **4** at the PMP2 level of theory. As a result, subsequent analyses of the dissociation of species **4** are restricted to the lowest-energy dissociation products **5** and **6** (see Figures 1 and 2).

The structure of species **4** contains features reminiscent of the dissociation products $HCaNH_2CH_3^+$ and CH_3. The N−Ca, Ca−H, and N−C bond lengths in **5** differ by no more than 0.013 Å from the equilibrium values obtained in **4**; in addition, the C−H distances and H−C−H bond angles of the quasi-planar CH_3 moiety of **4** are very similar to those of methyl radical **6**.

By contrast, the structure of species **4** contains profound differences from isomer **3**, the most noticeable being the presence of a Ca−H bond in **4** (1.986 Å) where only a small Ca−H interaction exists in **3** (Ca−H separation = 3.752 Å). This structural change is consistent with a hydrogen migration from the ammonium nitrogen in **3** to the calcium atom in **4**. In addition, **4** contains a stronger Ca−N interaction and a weaker Ca−C bond than in **3**, as well as an amino (rather than an ammonium) functional group. A more detailed understanding of the structural changes associated with the isomerization of **3** and **4** necessitates an examination of the charge and spin distributions of these species (see Figure 2), to be discussed further in Section B. 2.

The two minimum-energy isomers **3** and **4** are, in principle, interconvertible through the TS **7**, which we have also identified (although maximum gradient convergence only to −0.00352 hartrees/bohr was possible). A subsequent frequency calculation on this TS yielded one imaginary vibrational frequency (25i cm^{-1}), for which the most significant nuclear motion was a hydrogen migration between the amino nitrogen and the $CaCH_3$ calcium, in a manner consistent with interconversion of **3** and **4**. Species **7** (see Figure 2) contains a Ca−N distance (3.943 Å; not shown) intermediate between that of **3** (4.767 Å) and that of the dative bond in **4** (2.518 Å), a Ca−H distance (2.349 Å) intermediate between that of **3** (3.752 Å) and the Ca−H two-electron bond in **4** (1.986 Å), and a Ca−C separation (2.812 Å) between that of the Ca−C bond in **3** (2.405 Å) and that of the weak Ca−C interaction in **4** (2.954 Å). A more detailed discussion of the structural rearrangements required for this isomerization is given in Section IV.

However, the energy of **7** was found to be 21 kcal mol^{-1} above **3** (scaled ZPE included). As was mentioned earlier, the energy required to dissociate **4** into $HCaNH_2CH_3^+ + CH_3$ is only 8.17 kcal mol^{-1}, far below that required for isomerization over the TS to **3**. As species **3** itself is bound with respect to $CH_3NH_3^+ + CaCH_3$ only by 7.07 kcal mol^{-1} at this level, it is evident that, in the gas phase, both **3** and **4** are more likely to dissociate than to undergo interconversion. As a result, it can also be stated that **4** cannot be formed by the gas-phase reaction of $CH_3NH_3^+$ with $CaCH_3$ at thermal energies. Nevertheless, our calculations show that species **4** is bound, albeit by only 8.17 kcal mol^{-1} relative to its lowest-energy dissociation products, and its production in the gas phase should be possible under appropriate experimental conditions.

2. MP2 Level. On inclusion of electron correlation, the optimized structure of species **4** differs from its SCF-level counterpart in its "compactness" and in the position of the "migrated" hydrogen atom relative to the calcium atom to which it is bonded. At UMP2, the N−Ca dative bond is shorter by 0.047 Å (2.471 Å), the Ca−H bond is shorter by 0.032 Å (1.954 Å), and the Ca−C separation is shorter by 0.109 Å (2.845 Å) than at the SCF level. Furthermore, the bond angles that involve the Ca−H bond are considerably smaller [∠ N−Ca−H is smaller by 25.9° (103.5°); ∠ C−Ca−H is smaller by 9.2° (108.1°)]; in addition, ∠ C−N−Ca is 2.8° smaller (107.2°) than the SCF-optimized value. All of these geometric changes on proceeding from SCF to MP2 are consistent with a more compact structure at the correlated level of theory.

However, as stated earlier, species **4** is only weakly bound relative to dissociation products **5** and **6** (by 9.66 kcal mol^{-1} at PMP2; ZPE included; see Table 1 and Figure 1), and is more likely to dissociate in this manner than to isomerize to **3** via **7**. A UMP4SDTQ[20,26] single-point calculation at the SCF geometry obtained for **7** (see Table 1) yielded a PMP2 energy [with (s + 1) to (s + 4) spin contaminants annihilated] of −812.78986 hartrees, which is 33.36 kcal mol^{-1} above **4**, and is 20.98 kcal mol^{-1} above **3** (scaled ZPE included). As a full geometry optimization of **7** at UMP2 was found to be prohibitively expensive computationally, we report this result as an upper bound to the TS energy.

Analogous to what was found at the SCF level, species **4** contains structural features that are similar to each of dissociation products **5** and **6**. For example, **5** contains a dative N:→Ca bond, a conventional N−C bond, and a Ca−H bond, all of which are nearly identical in length to those found in **4**; also, the quasi-planar CH_3 moiety in **4** has similar bond lengths and bond angles to those found in the methyl radical **6**. In addition, the charge distributions, both in **4** and in **5**, show the calcium atom to support a large positive charge (q = +1.247 and q = +1.142, respectively); similarly, the spin densities in **4** and in **6** show the unpaired electron to reside on the planar or quasi-planar carbon atom (s = +1.164 and s = +1.277, respectively).

Whereas the positive charge in **4** lies on Ca, the unpaired electron is on the carbon atom adjacent to calcium (thus **4** is a distonic ion). Furthermore, the structure of the methyl group that contains this carbon atom is more reminiscent of a methyl

(26) (a) Krishnan, R.; Frisch, M. J.; Pople, J. A. *J. Chem. Phys.* **1980**, *72*, 4244. (b) Krishnan, R.; Pople, J. A. *Int. J. Quantum Chem.* **1978**, *14*, 91. (c) Frisch, M. J.; Krishnan, R.; Pople, J. A. *Chem. Phys. Lett.* **1980**, *75*, 66.

radical (see species **6** in Figure 2) than of a tetrahedral carbon-containing species such as methane. The existence of a Ca−N separation (2.471 Å) in **4** considerably longer than that obtained elsewhere for $Ca-NH_2$[10a,b,11b,h] but similar to that optimized for $Ca^{2+}\leftarrow{:}N{\equiv}N{:}$ (2.48 Å)[11a] suggests that the Ca−N interaction in **4** involves a dative bond (see Figure 2), which is consistent with the positive charge being on the calcium atom, rendering its 4sp hybrid orbital empty and thus available to form the N:→Ca dative bond.

Figure 5 displays the Ca−H, radical center CH_3, and N:→Ca molecular orbitals for species **4**. Figure 6 shows the Ca−H, N:→Ca, and radical-center CH_3 orbitals of the dissociation products $HCaNH_2CH_3^+$ (**5**) and $\bullet CH_3$ (**6**), and Figure 7 shows the highest-filled orbitals of the transition structure **7**.

The origin of the highest-filled molecular orbitals of **4** can be seen clearly from the orbital diagrams in Figure 6. The highest-filled orbital (ψ_{19}) of species **5** contains a large s-type lobe on the migrated hydrogen atom, and a smaller p-type lobe on the adjacent calcium atom, oriented toward this hydrogen atom. Clearly, this arrangement is representative of a Ca−H bond. The next highest-filled orbital (ψ_{18}) includes a large lobe on nitrogen, oriented toward calcium, indicative of a N:→Ca dative bond. The highest singly filled orbital on CH_3 (ψ_5^{α}) is an out-of-plane p_π -orbital centered on carbon.

Figure 7 displays the highest-filled MOs of transition structure **7**. The highest-filled orbital (ψ_{24}^{α}) contains a large lobe on the migrating hydrogen, a smaller p_π-lobe centered on the amino group, and a small lobe centered on calcium. Comparisons with the highest-filled orbitals in **3** (Figure 4), which contains three intact N−H bonds, and in **4** (Figure 5), which contains two intact N−H bonds and one intact Ca−H bond, indicate that ψ_{24}^{α} in **7** represents the process of N−H and valence−Rydberg bond breaking and Ca−H bond formation on proceeding from **3**, through **7**, to **4**. The next-highest-filled orbitals of **7**, ψ_{23}^{α} and ψ_{23}^{β}, provide a clear illustration of homolytic Ca−C bond cleavage during the isomerization of **3** to **4**. The α-component contains a p_π-lobe centered on the carbon atom of the CH_3 moiety adjacent to calcium; the β-component contains a diffuse lobe centered mainly on calcium, but delocalized to include the adjacent methyl carbon atom. These orbital pictures illustrate the homolytic cleavage of the C−Ca bond in **3**, resulting in one electron moving to a p_π-orbital of a CH_3 moiety within **4**; the other electron moves to contribute to a Ca−H bond in **4** (see Figures 2 and 5).

The next-highest-filled orbitals of **7**, ψ_{22}^{α} and ψ_{22}^{β}, display large lobes that are delocalized over the amino nitrogen and the migrating hydrogen, but also are oriented toward calcium. This orbital picture is reminiscent of ψ_{22}^{α} in **4** (see Figure 5), which represents a N:→Ca dative bond. Thus, ψ_{22} (the α-component of which is shown in Figure 7) appears to depict the process of N−H bond breaking and formation of a N:→Ca dative bond, as required to form **4** from **3**.

IV. Summary

We have performed ab initio MO calculations on structures associated with the bimolecular complexation of $CH_3NH_3^+$ (**1**) with $CaCH_3$ (**2**) to assess the feasibility of forming one-electron valence−Rydberg bonds between substituted calcium and NH_3 groups. Our investigation yielded the following results: (a) the ion−molecule complex (**3**) formed from initial contact of the two reactants is bound by 9.77 kcal mol^{-1} relative to $CH_3NH_3^+ + CaCH_3$ at the PMP2 level of theory; (b) the structure of **3** displays significant charge and spin delocalization between calcium and the adjacent ammonium group as well as a half-filled bonding orbital that involves both Ca valence and $R-NH_3^+$ Rydberg character.

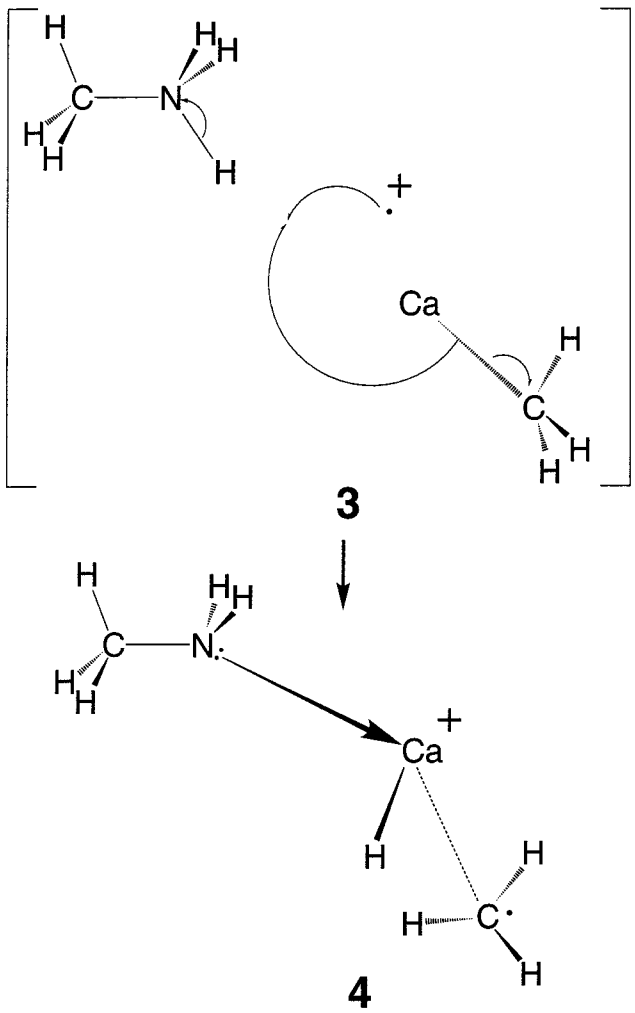

Figure 8. Electronic rearrangements associated with the interconversion of **3** and **4**.

These energetic and structural features are indicative of the formation of a weak one-electron bond between the 4sp hybrid valence orbital on calcium and a diffuse Rydberg orbital on the ammonium moiety.

Our studies also suggest the existence of a structural isomer (**4**) 12.38 kcal mol^{-1} below **3**. The formation of **4** from **3** requires substantial structural and bonding changes, as illustrated in Figure 8: (a) homolytic cleavage of the Ca−C bond, from which one electron contributes to the formation of a new Ca−H bond; the other electron occupies a p_π-orbital on a quasi-planar CH_3 moiety; (b) heterolytic cleavage of an ammonium N−H bond, from which the H^+ subsequently acquires hydridic character and forms a bond with calcium; (c) the unpaired electron on Ca in **3**, together with an electron from the cleaved Ca−C bond from **3**, combine with the migrating proton to form the Ca−H bond; (d) donation of a lone electron pair on nitrogen to calcium to form a dative Ca−N bond.

It must be emphasized that these rearrangements refer to a *concerted* process; by no means do we imply a stepwise mechanism when we enumerate the four changes that must occur.

Isomers **3** and **4** have been found to be interconvertible through transition structure **7**, which lies ca. 21 kcal mol^{-1} above **3**. However, as **3** is bound by only 9.77 kcal mol^{-1} relative to **1** and **2**, and **4** is bound by only 9.66 kcal mol^{-1} relative to **5**

and **6** (see Figure 1), it bears repetition that, in the gas phase, dissociation, rather than isomerization, is more likely to occur.

Acknowledgment. This work was supported by NSF grant no. CHE9618904. We also thank the Utah Center for High Performance Computing for computer and staff resources.

Supporting Information Available: Cartesian coordinates of species 1−7 as well as their energies at the SCF and MP2 levels of theory (PDF). This material is available free of charge via the Internet at http://pubs.acs.org.

JA992969X